



Improved Image Quality in Digital Mammography Using Anti-Scatter Grids

Samson O. Omondi^{1,2*}, Peter K. Msaki², Kazema R. Ramadhan³ and Innocent J. Lugendo²

¹Department of Radiography, College of Health Sciences, Jomo Kenyatta University of Agriculture and Technology, Nairobi, Kenya

²Department of Physics, University of Dar es Salaam, Dar es Salaam, Tanzania

³Department of Radiology and Imaging, Muhimbili University of Health and Allied Sciences, Dar es Salaam, Tanzania

*Corresponding author, E-mail: samomondi@jkuat.ac.ke; samkotieno@yahoo.com

Co-authors e-mail addresses: pmsaki@gmail.com; rkazema@hotmail.com;

ilugendo26@gmail.com

Received 1 July 2020, Revised 2 Sep 2020, Accepted 3 Sep 2020, Published Oct 2020

<https://dx.doi.org/10.4314/tjs.v46i3.4>

Abstract

Curability and effective management of breast cancer are dependent on its early detection. Early diagnosis strategies focus on providing timely access to breast cancer treatments by reducing barriers and improving access to effective early diagnosis. Mammography is the screening method of choice but suffers from degrading effects of scatter photons obstructing visualization of ductal carcinoma in situ and micro-calcifications in the breast. Quantitative evaluation of scatter suppression by anti-scatter grid using the beam stopper method has been investigated. Breast tissue equivalent phantom, polymethyl methacrylate was evaluated at X-ray mammographic nominal energy ranges. The anti-scatter grid used had aluminium interspace material and carbon fibre covers with varying grid features. Transmitted scatter and primary photon to the detector was analysed and evaluated. A scintillator type detector—model a Dexela 2315 MAM of size 290.8 × 229.8 mm having a resolution of 3072 × 3888 pixels was used. Transmitted scatter values in the range of 0.123 to 0.243 across the polymethyl methacrylate thickness of 10 mm to 80 mm were observed, whereas transmitted primary values recorded ranged from 0.713 to 0.495. Object, anti-scatter grid and X-ray energy exposure factors influenced the scatter fraction significantly. Improved mammography images showed significant improvements with this scatter reduction method using anti-scatter grid.

Keywords: Digital mammography, Anti-scatter grids, Breast screening, Scatter image artifacts, Beam stopper method.

Introduction

Breast cancer is the second leading cause of cancer deaths in women globally (Cumber et al. 2017, WHO AFRO 2020). The global risk factor of women above 40 years dying from breast cancer is about 1 in 38 (about 2.6%) and is on the increase. Breast cancer is the leading cancer amongst African women before cervical cancers compared to

the European women where lung cancer leads (WHO 2019). According to the prevalence and situational analysis by Cumber et al. (2017), the survival rates of breast cancer in Sub Saharan Africa are less than 40% compared to the developed countries with survival rates above 86%. The reason for the low five-year survival rates in Sub Saharan Africa is that most cancers are diagnosed at

advanced stages at first presentation (Cumber et al. 2017). Breast cancer screening is among the strategy for reducing the proportion of patients who are diagnosed at late stage. Mass screening of the asymptomatic and vulnerable populations is considered the most viable method of early detection of breast cancer. There are several approaches used for this purpose, but mammography is the most reliable method used for breast cancer (Pisano et al. 2005).

While screening by mammography has been successful in developed nations, in Sub Saharan Africa this intervention has not been that effective. This is inevitable because there are several factors that make mammography ineffective in early detection of breast cancer. These include low awareness levels of need for screening, limited access to mammography units, inadequate number of skilled personnel and inherent factors that make mammography ineffective (Pisano et al. 2005, Cumber et al. 2017). The effectiveness of mammography depends on the diagnostic quality of images (mammograms) produced and the reduced X-rays dose to the breast. Image quality improvement while reducing radiation dose to the breast using mammographic anti-scatter grids is an area of active research today after replacing the air gaps approach (Barnes and Brezovich 1978, Chan and Doi 1982, Dance and Day 1984, Rezentes et al. 1999, Boone and Cooper III 2000, Boone et al. 2000, Al Kafi et al. 2009, Zhou et al. 2016).

There are several factors that degrade the quality of mammograms used for breast cancer screening. These include breast positioning, inhomogeneity in tissue thickness, selection of exposure factors and scatter. Scatter degrades the image quality by reducing contrast, producing streaks, artifacts and cupping effects on images. These effects combine to impede diagnosis of ductal carcinoma in situ (DCIS), pathology in micro-calcifications and parenchymal breast tissues. The degrading effect of scatter on

mammograms being so severe, minimization of these effects is an area of active research (Boone et al. 2000, Al Kafi et al. 2009, Zhou et al. 2016, Zhou et al. 2018). There are two approaches to minimize the effects of scatter: scatter suppression before reaching the image receptor and subtraction methods after image formation. The scatter suppression approach has been studied by various researchers (Floyd et al. 1991, Boone et al. 2000, Al Kafi 2009, Zhou et al. 2016). However, quantitative methods for optimal factors before and during photons interactions influence on scatter reduction across the anti-scatter grids have not been much reported. Of interest in this work, is scatter preventive approach which is used to improve image quality while reducing patient dose.

Materials and Methods

Ethical consideration

Ethical clearance and permission was obtained from the Muhimbili National Hospital (MNH) Research Ethics Committee (MNH-REC Reference No. MNH/TRCU/permission/2020/123 and Ethical clearance certificate number MNH/IRB/1/2020/007). Permission was granted for access to the Radiology department both at MNH-Upanga and MNH-Mloganzila institutions by the Directorate of research.

Influence of anti-scatter grid features on scatter transmission to the image receptor

The anti-scatter grid used in this work for scatter reduction was mostly based on X-rays interaction features discussed by Chan and Doi (1982). The X-rays before detection undergo different interactions mechanisms in the object and anti-scatter grid. The desired image is formed by the primary photons which are often severely degraded by the scattered photons from the object and anti-scatter grid. The features of the anti-scatter grid assembly that have influence on the scatter include: the size and material of the interspace, grid height, the septa thickness,

septa frequency and grid ratio. As indicated in Table 1, these features are usually determined by the manufacturers. For the sake of comparison, the features of the mammographic anti-scatter grid used in this work (Genoray DMX 600) and one used in a previous work by Carton et al. (2009) (Smit

Röntgen) have been listed in Table 1. The common scatter reduction features of both mammographic grids are the grid ratio, septa thickness and material of septa. Therefore, based on these features they will have comparable scatter reduction capabilities.

Table 1: Properties of two mammographic anti-scatter grids fitted in Smit Röntgen (previous work) and Genoray DMX 600 (this work) are presented

Grid properties	Smit Röntgen	Genoray DMX 600
Grid ratio r ,	5:1	5:1
Lead to interspace ratio (R)	0.0667	0.0778
Septa thickness d (cm)	0.0020	0.0020
Septa material	Lead	Lead
Inter-space distance D (cm)	0.0300	0.0257
Inter-space material	Fibre	Aluminium
Septa frequency N (cm ⁻¹)	31	36
Focal distance f_0 (cm)	65	65
Cover material	Fibre	Carbon fibre
Grid total cover thickness (cm)	0.0400	0.0350
Septa height h (cm)	0.1500	0.1285
Maximum source to grid distance (SGD) (mm)	650	650

Because of its many features, the anti-scatter grid Genoray DMX 600 used in this study is expected to be more effective in scatter reduction. These include; interface material, septa height, high septa frequency and interspace distance. In order to assess the effectiveness of the anti-scatter grid in scatter suppression, the measurements were done as described below.

Experimental set up

The experimental set up followed protocols of the International Electrotechnical Commission (IEC) standards 60627 (IEC 2013) for radiation measurements with and without anti-scatter grids. The experimental set up showing the X-ray source, object, anti-scatter grid and the detector used in this work is shown in Figure 1.

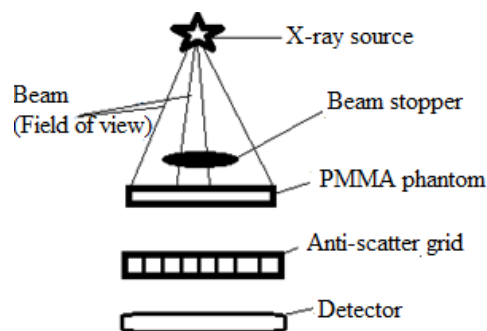


Figure 1: Experimental set-up of the imaging geometry.

Influence of object thickness on scatter

Evaluation of the influence of object thickness on the generation and transmission of scattered X-rays through mammographic phantoms, anti-scatter grid to the image receptor was done. Breast tissue equivalent phantoms, polymethyl methacrylate (PMMA) mammographic phantoms of 23.0 x 29.2 cm² cross-section area in 10 mm thickness sheets

were used. The PMMA sheets in incremental steps of 10 mm thickness each were successively placed on the clamp and exposed up to 80 mm. To quantify the scatter transmission by the beam stopper method, two sets of measurements were made. The first set of measurements was the broad beam condition with the beam stopper in place to determine the transmitted scatter (Ts). The second set of measurements to determine the total photon transmission (Tt) was a broad beam condition without the beam stopper in place. In order to assess the effectiveness of this method, an additional measurement was made to determine the transmitted primary photons (Tp) by setting up narrow beam condition. For each condition, measurements were repeated six times and the mean determined. In all the measurements, a Dexela 2315 MAM detector with resolutions of 3072 x 1944 pixels fitted in the Genoray DMX 600 digital mammography unit was used. It was a flat panel detector operating on a complementary metal-oxide semiconductor (CMOS) with high detective quantum efficiency (DQE), high speed and low noise X-ray detection with an excellent sensitivity. The images were automatically transferred to the picture archiving and communication system (PACS) distribution system for archiving and storage where they were later sent to the work stations for analysis.

Influence of photon beam on scatter

A number of factors affect the amount of scatter produced during X-ray interactions in the object. Two main X-ray beam factors to be evaluated are, energy (kVp) and the field of view (FOV) size. The Genoray DMX 600 installed at MNH-Mloganzila had an inherent filtration of 0.55 Be (IEC 60522) whose target material operates clinically at Mo/Mo (at lower kVp) and molybdenum-rhenium(Mo/Rh) for the higher kVp values. The unit has optimal energy range of 22-39 kV allowing for manual and automatic exposure control (AEC) selection options. The anti-scatter grid installed in this unit had

the following features: grid ratio 5:1, lead septa of thickness of 0.0020 cm, septa frequency of 36 lines/cm, aluminium interspace material of distance 0.0257 cm and carbon fibre covers of total thickness 0.0350 cm and focal distance of 65 cm.

Results and Discussion

Influence of phantom thickness on scatter estimated

Estimation of photon transmission through the anti-scatter grid by the beam stopper method with a beam stopper in place (Ts) and without (Tt) for various PMMA phantom thicknesses are presented in Table 2. Tp which was obtained by subtracting Ts from Tt is also shown.

Table 2: Recorded mean of the Ts, Tt and Tp as a function of PMMA thickness exposed at 33 kVp in fixed field of view

PMMA thickness (mm)	Tt (Mean)	Ts (Mean)	Tp (Mean)
10	0.836	0.123	0.713
20	0.830	0.210	0.620
30	0.827	0.211	0.616
40	0.813	0.219	0.594
50	0.801	0.224	0.577
60	0.796	0.238	0.558
70	0.782	0.240	0.542
80	0.738	0.243	0.495

From Table 2, the decrease of primary photons transmission with the increasing PMMA thickness is less pronounced than the increase of scatter transmission. At a fixed kV, Ts is seen to increase with PMMA thickness from 8.7% to 12% for thicknesses of 10 mm to 80 mm of PMMA phantom, respectively. The variations of Ts and Tp with thickness shown in Table 2, indicate that correction for scatter is more important than attenuation correction in mammographic techniques. It is also evident from Table 2 that, the methods used for estimation of scatter at diagnostic X-ray energies are comparable. Therefore, both quantitative

methods for scatter estimation can be used interchangeably. What is not clear in this study is the accuracy of the scatter estimation method. However, using Pearson correlation coefficient of Ts and Tp, a perfect correlation

was obtained as shown in Figure 2. This means the scatter estimation by this quantitative beam stopper method is accurate.

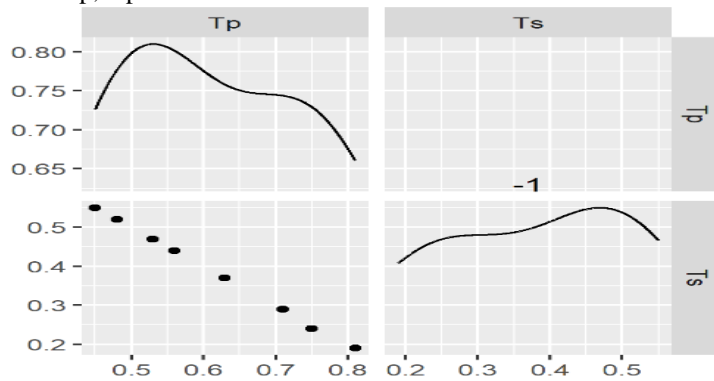


Figure 2: Pearson correlation coefficient between Tp and Ts.

While both methods estimate Ts and Tp accurately, they do not have ability to discriminate the origins of scatter, which, in this case, scatter from the object and the anti-scatter grid. These limitations can be overcome by scatter estimation by the Monte Carlo simulations.

The images of two sets of mammograms obtained at similar irradiation conditions of

33 kVp and same field of view size (23.0 x 29.2) cm² by Genoray DMX 600 mammography unit for different thicknesses of PMMA breast tissue equivalent phantoms (30 mm and 80 mm) are shown in Figure 3. Images 3(a) and (b) are formed by Tt (scatter uncorrected) and 3(c.) and (d) are formed by Tp (scatter corrected).

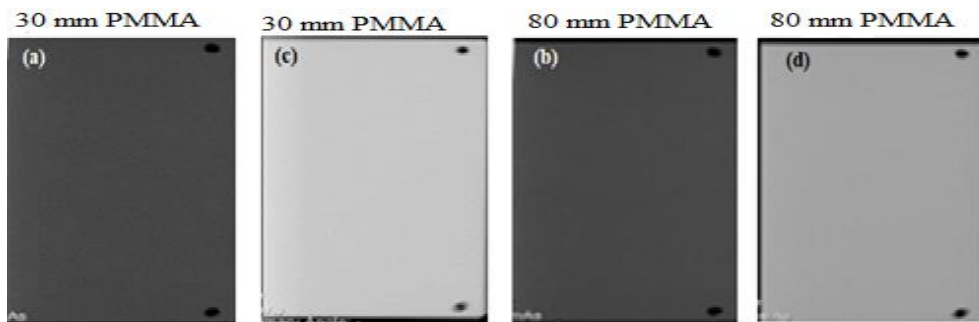


Figure 3: Mammograms obtained by irradiating PMMA phantoms of different thicknesses.

The contrast difference between uncorrected and corrected images in Figure 3 is clearly demonstrated. This is because the primary photons forming the images are not significant and shadowed by transmitted scatter. However, contrast enhancement by scatter correction is more pronounced in

Figure 3 (d), indicating that the scatter suppression is more effective for breast tissue equivalent phantom of larger thickness. The loss of contrast on the images in mammography by scatter is undesirable because it impedes visualization of intended diagnostic imaging result.

Dependence of scatter fraction on the thickness of PMMA phantoms

Most studies use scatter fraction (SF) which is a measure of the portion of scatter in the total measured radiation energy deposited

on the detector for evaluating the effectiveness of scatter correction techniques. SF values as ratios of T_s and T_t from Table 2 have been evaluated and plotted in Figure 4 as a function of phantom thicknesses.

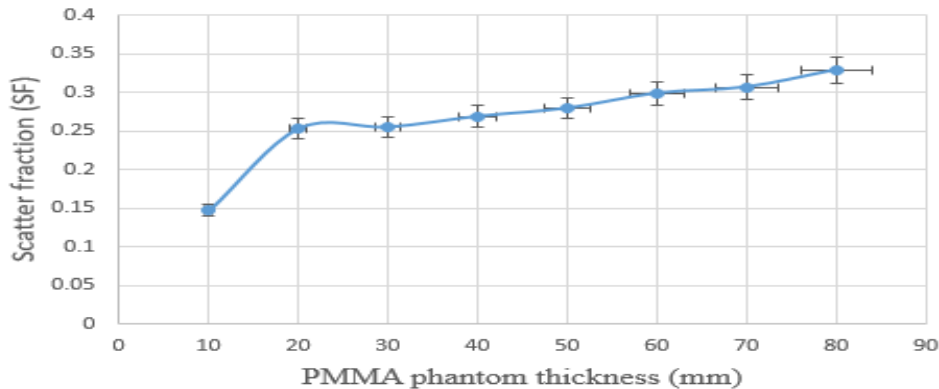


Figure 4 The scatter fraction (SF) against PMMA phantom thickness at a fixed spectral kVp.

From Figure 4, there is a sharp increase in the scatter fraction from 0.15 at 10 mm to 0.25 at 20 mm phantom thickness. After 20 mm phantom thickness scatter increases nearly gradually to above 0.34. From these observations, it is evident that the need for scatter correction increases rapidly with PMMA phantom thickness up to 20 mm. After 20 mm thickness, the need for image scatter correction remains nearly constant.

Influence of mammographic X-ray beam on scatter

In the previous section, the influence of phantom factors on scatter have been discussed. In this section, the influence of the spectra kVp and field of view on scatter are presented. Dependence of T_s and T_p on the energy of X-ray spectra obtained from the narrow beam stopper method is plotted as a function of the lower and higher energy in Figure 5. According to Figure 5, there is a weak dependence of T_s on X-ray spectra for the entire range of energy commonly used in mammography. This energy dependency has also been reported in previous studies by Boone et al. (2000). However, the

dependency of scatter on energy is not precise because the kVp used suffers from poly-energetic beam effects. This limitation associated with the beam effects can be overcome by simulation of monochromatic spectra kVp.

The influence of FOV on scatter fraction for the default FOV and (15 x 12.5)–FOV as a function of PMMA phantom thickness is shown in Table 3. It is observed from this table that scatter fractions increase both with phantom thickness and FOV.

From Table 3, the default maximum FOV-(23.0 x 29.2) cm of the DMX 600 mammography unit shows relatively higher scattered fractions than the (15.0 x 12.5) cm–FOV. The scatter fractions vary from 0.423 to 0.689 for 10 mm and 80 mm PMMA phantom thickness, respectively for (23.0 x 29.2) cm–FOV compared to 0.376 to 0.547 over the same thicknesses for (15.0 x 12.5) cm–FOV. Since the scatter fraction values varying from 0.376 to 0.689 for both FOVs are high, scatter correction is imperative if high quality images obtained by these FOVs are desired.

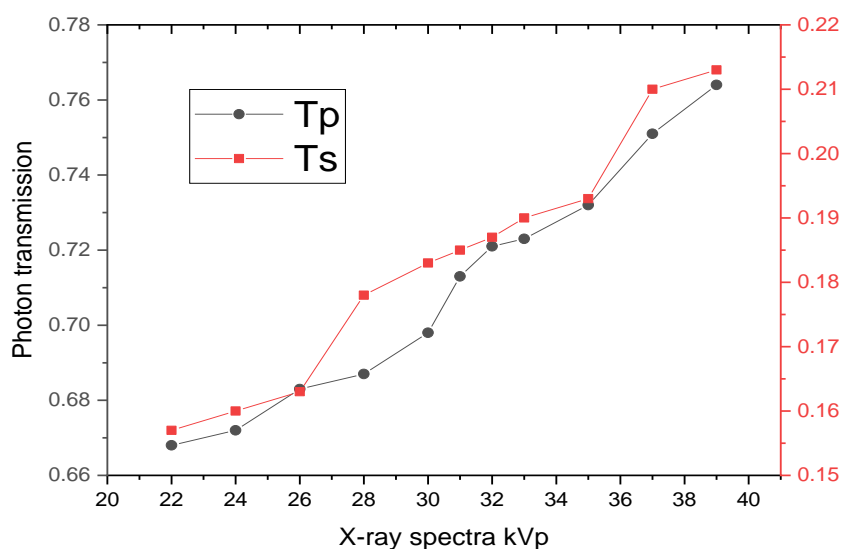


Figure 5: The relationship between the transmission of photons (primary and scatter) versus the X-ray spectra (kVp) through a 20 mm PMMA phantom thickness.

Table 3: Scatter fractions versus the field of view size (FOV) at 34 kVp

Thickness of PMMA phantom (mm)	(23.0 x 29.2) cm-FOV	(15.0 x 12.5) cm-FOV
10	0.423	0.376
20	0.431	0.398
30	0.456	0.418
40	0.478	0.445
50	0.505	0.454
60	0.578	0.489
70	0.603	0.523
80	0.689	0.547

Conclusion

Scatter is the major image degrading factor in soft tissue X-ray imaging. Scatter is enhanced by the size or thickness of tissues, the field of view size and the X-ray energy. It is observed that for mammographic X-ray imaging, scatter correction is of utmost importance than attenuation correction. Quantitative scatter correction methods, however, cannot discriminate the scatter from the object and those from the anti-scatter grid assembly. From this study therefore, it is concluded that the effective scatter suppression by use of the

anti-scatter grids should be coupled with a careful evaluation of anti-scatter grids features, object thickness and X-ray spectra factors. Therefore, these factors if carefully selected for digital mammography, they have been shown in this work to improve image quality.

Conflict of Interest: The authors declare that they have no conflict of interest. The authors are responsible for the content of this paper.

Acknowledgements

The authors acknowledge Jomo Kenyatta University of Agriculture and Technology (JKUAT) for the study leave that was granted to the first author and the management of Muhimbili National Hospital for granting access, ethical clearance and permission to use X-ray imaging facilities. We are indebted to the radiographers in charge Mr. Boniface and Mr. Mzeru of MNH-Upanga and MNH-Mloganzila, respectively, for their technical assistance. We appreciate the support of biomedical engineers of the two facilities. Finally, we sincerely acknowledge the financial support granted for this study by Breaking Limits Enterprises owned by Mrs. Lilian Omondi who made resources available towards the tuition fees, research funds, accommodation and subsistence during the study period.

References

- Al Kafi MA, Maalej N and Naqvi AA 2009 Scatter dose calculation for anti-scatter linear grids in mammography. *Appl. Radiat. Isot.* 67: 1837-1841.
- Barnes GT and Brezovich IA 1978 The intensity of scattered radiation in mammography *Radiol.* 126: 243-247.
- Boone JM and Cooper III VN 2000 Scatter/primary in mammography. Monte Carlo validation. *Med. Phys.* 27: 1818 - 1831.
- Boone JM, Lindfors KK, Cooper III VN and Seibert AJ 2000 Scatter/primary in mammography: comprehensive results. *Med. Phys.* 27: 2408-2416.
- Carton A-K, Acciavatti R, Kuo J and Maidment ADA 2009 The effect of scatter and glare on image quality in contrast-enhanced breast imaging using a-Si/CsI full-field flat panel detector. *Med. Phys.* 36: 920-928.
- Chan H-P and K Doi 1982 Investigation of the performance of anti-scatter grids: Monte Carlo simulation studies. *J. Phys. Med. Biol.* 27: 785-803.
- Cumber SN, Nchanji KN and Tsoka-Gwegweni JM 2017 Breast cancer among women in Sub-Saharan Africa: prevalence and situational analysis. *S. Afr. J. Gynaecol. Oncol.* 9: 35-37.
- Dance DR and Day GJ 1984 The computation of scatter in mammography by Monte Carlo methods. *Phys. Med. Biol.* 29: 237-247.
- Floyd Jr. CE, Lo JY, Chotas HG and Ravin CE 1991 Quantitative scatter measurements in digital radiography using a photostimulable phosphor imaging system. *Med. Phys.* 18: 408-413.
- IEC (International Electrotechnical Commission) 2013 Diagnostic X-ray imaging equipment: Characteristics of general purpose and mammographic anti-scatter grids. 3.0. ed. Geneva: IEC
- Pisano ED, Gatsonis C, Hendrick E, Yaffe M, Baum JK, Acharyya S, Conant EF, Fajardo LL, Bassett L, D'Orsi C and Jong R 2005 Diagnostic performance of digital versus film mammography for breast-cancer screening. *New Engl. J. Med.* 353(17): 1773-1783.
- Rezentes PS, de Almeida A and Barnes GT 1999 Mammography grid performance. *Radiol.* 210: 227-232.
- WHO (World Health Organization) AFRO 2020 Cancer statistics 2020 WHO Geneva.
- WHO 2019 Country profiles 2019, WHO Geneva.
- Zhou A, Yin Y, White GL and Davidson R 2016 A new solution for radiation transmission of anti-scatter grids. *Biomed. Phys. Eng. Express* 2: 055011.
- Zhou A, White GL and Davidson R 2018 Validation of Monte Carlo code system for grid evaluation with interference effect on Rayleigh scattering. *Phys. Med. Biol.* 63(3): p.03NT02.